



Gamma-radiation-induced negative nonlinear absorption in quartz glass

February 2022

Changing the World's Energy Future

Bryan W. Morgan, Milos Burger, IGOR JOVANOVIC, MATTHEW P. VAN ZILE, Piyush Sabharwall



DISCLAIMER

This information was prepared as an account of work sponsored by an agency of the U.S. Government. Neither the U.S. Government nor any agency thereof, nor any of their employees, makes any warranty, expressed or implied, or assumes any legal liability or responsibility for the accuracy, completeness, or usefulness, of any information, apparatus, product, or process disclosed, or represents that its use would not infringe privately owned rights. References herein to any specific commercial product, process, or service by trade name, trade mark, manufacturer, or otherwise, does not necessarily constitute or imply its endorsement, recommendation, or favoring by the U.S. Government or any agency thereof. The views and opinions of authors expressed herein do not necessarily state or reflect those of the U.S. Government or any agency thereof.

Gamma-radiation-induced negative nonlinear absorption in quartz glass

**Bryan W. Morgan, Milos Burger, IGOR JOVANOVIĆ, MATTHEW P. VAN ZILE,
Piyush Sabharwal**

February 2022

**Idaho National Laboratory
Idaho Falls, Idaho 83415**

<http://www.inl.gov>

**Prepared for the
U.S. Department of Energy
Under DOE Idaho Operations Office
Contract DE-AC07-05ID14517**

Gamma-radiation-induced negative nonlinear absorption in quartz glass

BRYAN W. MORGAN,^{1,*}  MATTHEW P. VAN ZILE,² PIYUSH SABHARWALL,^{1,3} MILOS BURGER,^{1,4} AND IGOR JOVANOVIĆ^{1,4}

¹Department of Nuclear Engineering and Radiological Sciences, University of Michigan, Ann Arbor, MI 48109, USA

²Nuclear Reactor Laboratory, The Ohio State University, Columbus, OH 43212, USA

³Idaho National Laboratory, Idaho Falls, ID 83415, USA

⁴Gérard Mourou Center for Ultrafast Optical Science, University of Michigan, Ann Arbor, MI 48109, USA

*bryanmo@umich.edu

Abstract: The effect of ionizing radiation on the nonlinear optical properties of materials needs to be considered for applications that employ high-power laser pulses in extreme radiation environments. The Heraeus Infrasil302 optical quartz glass was irradiated by gamma rays, and its nonlinear absorption was measured using the open-aperture Z-scan technique with nanosecond laser pulses. Irradiation results in a negative nonlinear absorption coefficient whose magnitude increases with irradiation dose. Nonlinear absorption coefficients of -0.78 , -1.14 , -1.29 , and -1.88×10^{-13} m/W are measured for gamma doses of 600 krad, 1.2 Mrad, 3.6 Mrad, and 10 Mrad, respectively. Thermal annealing restores the optical properties of quartz-glass to their unirradiated values. It is suggested that metallic impurities introduced by the manufacturing process have a role in inducing saturated absorption in irradiated quartz glass, which manifests as negative nonlinear absorption coefficient, and is demonstrated by comparing Infrasil302 quartz results to equivalent irradiated measurements for Spectrosil2000 quartz.

© 2022 Optica Publishing Group under the terms of the [Optica Open Access Publishing Agreement](#)

1. Introduction

The performance of optical materials in extreme radioactive and thermal environments is important for the development of applications such as optical instrumentation for fission power reactors, fusion energy, accelerator-based research, and space-based systems. Irradiated optical materials are altered at the atomic and molecular scale, which manifests macroscopically as radiation-induced absorption and refractive index change [1–3]. The physical origin of material's polarizability suggests that these radiation-induced changes of the linear optical properties could be accompanied by changes in the material's nonlinear refractive index and nonlinear absorption. Both the linear and nonlinear effects may significantly impact the operation of optical systems, *e.g.* by altering the transmitted laser energy or by optical damage through catastrophic self-focusing. A more complete understanding of the impact of ionizing radiation on the optical properties, including the material's nonlinear optical response, is necessary to select appropriate materials for applications in extreme radioactive environments.

A change in nonlinear optical absorption alters the total absorption coefficient and, thus, the transmitted energy dependent on the applied intensity, which can be described as

$$\alpha = \alpha_0 + \beta I_0. \quad (1)$$

Here, α_0 is the linear absorption coefficient, I_0 is the light intensity, and β is the nonlinear absorption coefficient that accounts for the simultaneous effects of two-photon absorption (TPA) and saturable absorption (SA) [4]. Altering the material's nonlinear absorption may have significant impact in applications that require precise power and intensity control of light sources, or that use the optical beam power or intensity for analytical purposes.

Multiple physical processes contribute to the cumulative nonlinear effects observed in an optical material, including multiphoton absorption, SA, excited-state absorption, electrostriction, and thermal effects [4–6]. These processes exhibit dependence on the laser irradiance, fluence, and energy. TPA is a form of ultrafast third-order nonlinearity, whereas SA is a cumulative or slow nonlinear effect [4,7]. The Z-scan technique is frequently used to measure a material's nonlinear properties [8]; Z-scans performed in the nanosecond regime are sensitive to both ultrafast and slow nonlinearities. TPA is the dominant and well-studied ultrafast third-order nonlinear susceptibility that is observed both in the traditional optical media and in semiconductors [4,9–12]. The slow nonlinearity that accompanies SA is observed in semiconductors, nanocomposites, thin films, and doped glasses, but not in undoped bulk optical media such as fused silica, quartz, and sapphire [9,11–15]. In the presence of both TPA and SA, their competition determines the effect of the increasing intensity on the magnitude of nonlinear absorption. SA occurs when the saturation intensity, I_S , is exceeded, resulting in the *Pauli blocking* effect: the material's available higher electron energy states are filled due to photoelectric absorption, and further photon absorption is constrained [14]. The SA coefficient, α_{SA} , is defined by [6,13,14].

$$\alpha_{SA} = \frac{\alpha_0}{1 + I_0/I_S}. \quad (2)$$

Here we report the observation of nonlinear absorption in quartz glass induced by gamma irradiation. The measurements were performed using an open-aperture Z-scan method in the nanosecond regime. The nonlinear absorption coefficient was measured for 600 krad, 1.2 Mrad, 3.6 Mrad, and 10 Mrad irradiation doses and shows a monotonic increase with radiation dose. Thermal annealing at 400 °C is shown to restore the quartz glass to its unirradiated nonlinear optical characteristics, similar to the effect of annealing on linear absorption. Concurrent-irradiation thermal annealing at 800 °C was also shown to anneal the Infrail302 completely to its unirradiated state.

2. Experiment

The nonlinear absorption of quartz glass was measured by the open-aperture Z-scan technique using ~10-ns laser pulses [4,8]. Sample irradiations were performed by ^{60}Co , which produces 1.17-MeV and 1.33-MeV gamma rays at an average dose rate in Si of $12.05 \text{ krad} \cdot \text{hr}^{-1}$ inside the sample heating furnace. For radiation protection, the irradiations took place in a water pool located at the Ohio State University's Nuclear Reactor Laboratory and at the Pennsylvania State University's Radiation Science and Engineering Center. Subsequent to irradiation, samples were heated in custom-fabricated silicon-carbide insulated furnaces to examine the effect of thermal annealing on optical properties. Irradiations were also performed with concurrent-irradiation thermal annealing for comparison to the unheated irradiation results.

The Z-scan experiment, shown in Fig. 1, is based on similar prior designs and is described in greater detail in our previous work [16]. The setup is compact and self-contained, such that it can be easily relocated adjacent to the site of irradiation, which minimizes the time between sample irradiation and post-irradiation examination. The Z-scan experiments were performed using the 532-nm second harmonic of a nanosecond pulsed Nd:YAG laser. In the nonlinear absorption measurement, the laser pulse power is measured as the sample transits the laser focus using a “reference” sensor before the optical sample, and an “open-aperture” sensor after the optical sample, as shown in Fig. 1. The ratio of the laser power transmitted through the sample to the reference laser power measured before the sample is plotted against the position as the sample is translated through the laser focus to obtain the characteristic open-aperture Z-scan curve. The measured curve is fit to model to extract the nonlinear absorption coefficient. “Closed-aperture” measurements may also be simultaneously performed with a second sensor and aperture to measure the nonlinear refractive index.

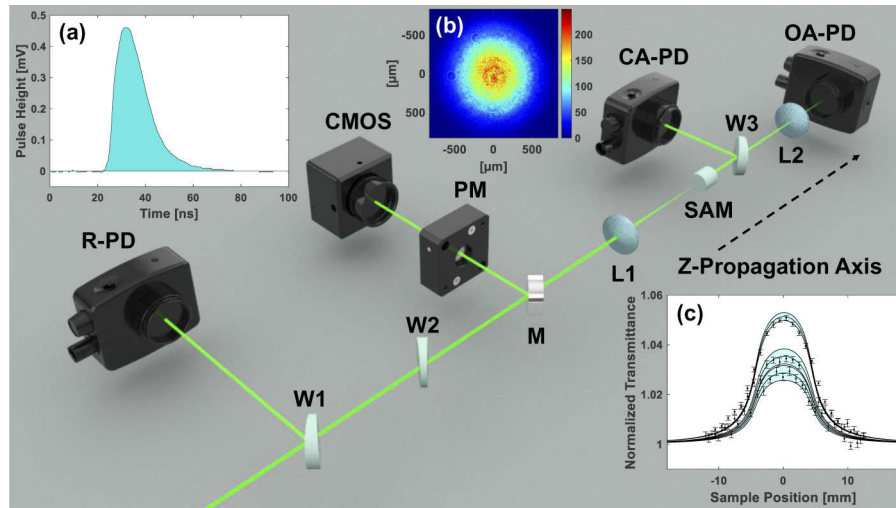


Fig. 1. Z-scan experiment after spatial filtering: optical wedges (W1–3), the reference (R-PD), closed-aperture (CA-PD) and open-aperture (OA-PD) photodiodes, power meter (PM) and CMOS camera after a removable mirror (M), focusing lenses (L1, L2), and the optical sample (SAM) under examination. Inset: (a) an example pulse time profile, (b) spatially filtered laser beam profile, and (c) normalized transmittance curves obtained by the ratio of the OA-PD to the R-PD during an open-aperture Z-scan measurement.

An example of a Z-scan nonlinear absorption measurement of NBK7 glass used for calibration can be seen in Fig. 2. In all Z-scan plots the error bars are the error on the mean (standard error), and the magenta shaded area is the error propagated variation in the least squares fit. The normalized transmittance in the figure is the ratio of the laser power transmitted to the open-aperture sensor after the sample to the power transmitted by the laser to the reference sensor before the sample. By convention, the transmittance is normalized to unity when the sample is far from focus. As the sample approaches focus during the Z-scan, a positive nonlinear absorption coefficient results in a decrease in transmission through the sample, indicated by the decrease in the normalized transmittance. In contrast, a negative nonlinear absorption coefficient would result in an increase in transmittance as the sample approaches the laser focus, producing a rise in the Z-scan normalized transmittance curve.

Figure 3 shows the annealing furnace that the samples are contained within during irradiation in the ^{60}Co dry tube and the silica-based sample mounting hardware for suspending the samples within the furnace. The furnace is custom fabricated for insertion into the dry tube to allow for thermal annealing samples while they are being irradiated, or to heat the samples post-irradiation. The window samples are stacked within the white silica sleeve shown in Fig. 1(b), which is suspended within a silica glass tube to physically separate the samples from the furnace heating coil. The samples within the silica tube are then inserted vertically within the coiled heating element within the white insulated portion of the heater shown in the yellow box of Fig. 3(a). Two thermocouples were mounted to the sample silica sleeve, adjacent to the samples within the silica glass tube, to monitor temperature and ensure the samples do not overheat. The ambient temperature within the furnace inside the ^{60}Co dry pool was measured to be 20 °C and is assumed constant throughout the unheated irradiations.

Prior to each irradiation, the quartz glass sample was measured by Z-scan, and the sample was measured again immediately after irradiation. The sample was then thermally annealed post-irradiation at 200 °C, 400 °C, 600 °C, and 800 °C, for 30 minutes at each temperature. After each annealing step the sample was again evaluated by Z-scan. For concurrent-irradiation thermal

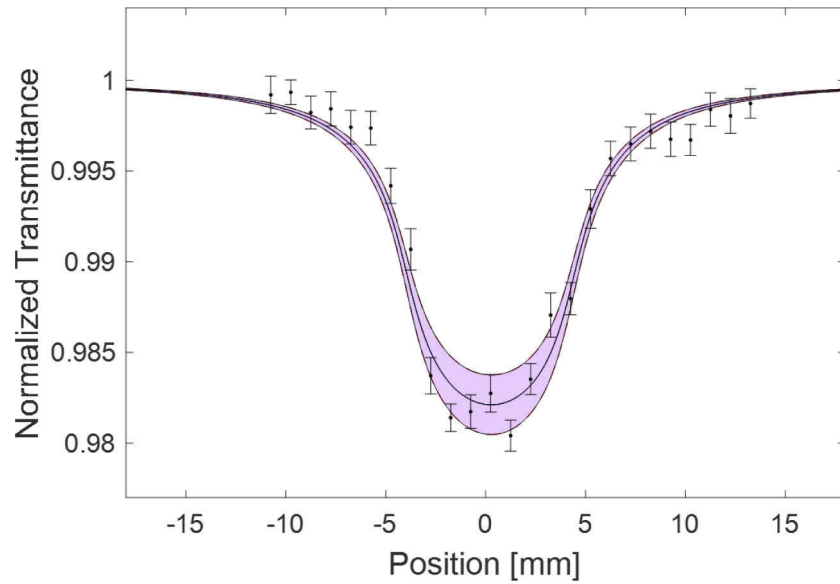


Fig. 2. Example Z-scan calibration nonlinear absorption measurement of NBK7 yielding $\beta = (2.71 \pm 0.25) \times 10^{-14} \text{ m/W}$.

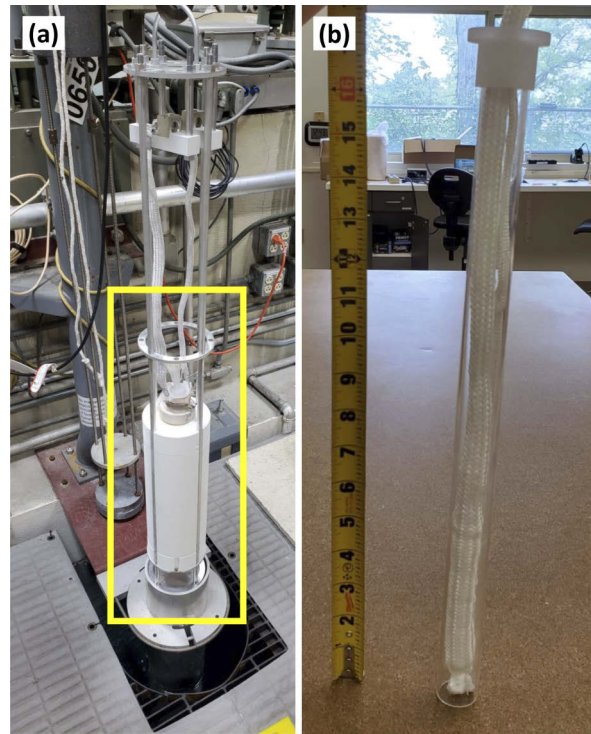


Fig. 3. (a) Custom-fabricated furnace for sample insertion into the ^{60}Co pool dry tube and concurrent thermal annealing. The furnace is suspended for insertion into the ^{60}Co dry tube. The silicon carbide heating element and silica-alumina insulation are denoted by the yellow box. (b) Fused silica tube and silica sleeve that suspend the window samples within the furnace's silicon carbide heating element and alumina insulation during irradiation.

annealing experiments the samples were heated to 800 °C for the duration of the irradiation. Linear absorption measurements of the quartz glass sample were performed at each irradiation step using a DH-2000-BAL Ocean Insight light source and an HR-4000 CG-UV-NIR Ocean Insight spectrometer. The light source and spectrometer were coupled to the sample through 600- μm diameter solarization resistant fibers and two collimating lenses mounted to a static sample holder. The linear absorption was measured over a range of 200–1100 μm . The optical density, $OD = (1/L) \log_{10} (I_0/I_S)$, is obtained by measuring the reference transmission spectrum of the DH-2000 light source without a test sample present, I_0 , and then measuring the transmission spectrum again with an optical test sample inserted into the holder, I_S , and dividing by the sample depth L . The measured stability of the DH-2000 BAL as a function of time was 0.01 % h^{-1} at 254 nm and 700 nm. A reference measurement was taken for every transmission measurement so that the reference and sample spectra were measured within 5 minutes of each other.

3. Results

The nonlinear absorption of Infrasil302 optical quartz glass was measured before irradiation and following gamma irradiations to 600 krad, 1.2 Mrad, 3.6 Mrad, and 10 Mrad. It was then measured again after each thermal annealing step, as described in the experimental section. Figure 4 shows the Z-scan nonlinear absorption curves measured for quartz glass before irradiation and immediately after each of the four gamma irradiations. The unirradiated nonlinear absorption coefficient of quartz glass is $5 \times 10^{-15} \text{ m/W}$, which is too small for our system to detect [9]. A negative nonlinear absorption coefficient is measured following all four irradiations, and its magnitude increases with dose. The negative nonlinear absorption coefficient persists after annealing to 200 °C, as seen in Fig. 5. The sample exhibited its pre-irradiation nonlinear absorption after annealing to 400 °C. Two Infrasil302 samples were used throughout these measurements. The first sample was irradiated to 600 krad, and the results are presented in Figs. 4(b) and 5(a). A second Infrasil302 sample from the same batch was used for the 1.2 Mrad, 3.6 Mrad, and 10 Mrad irradiations with post-irradiation thermal annealing. The use of two Infrasil302 samples from the same batch demonstrates repeatable radiation-induced negative nonlinearity across multiple Infrasil302 samples from the same batch. The second Infrasil302 sample used also shows that the nonlinearity can be induced by repeated irradiation following the thermal annealing.

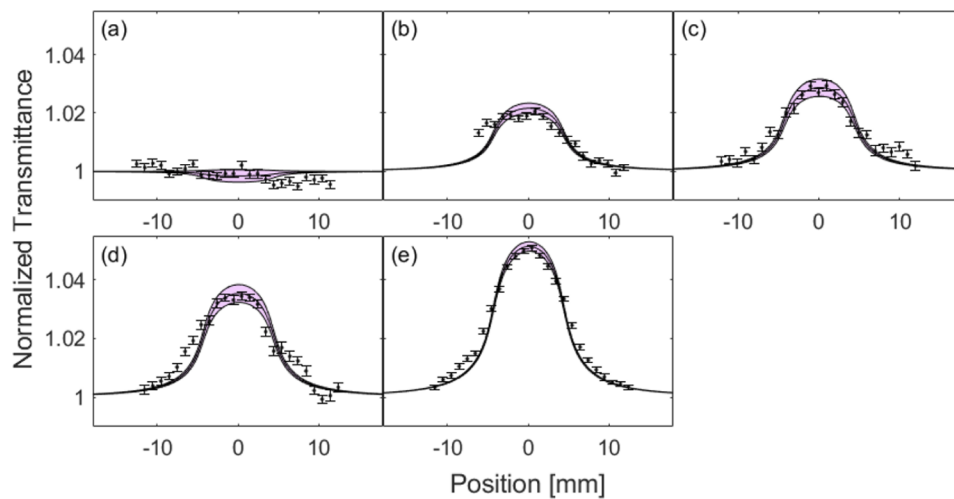


Fig. 4. Open-aperture Z-scan measurements of Infrasil302 (a) unirradiated, (b) 600 krad, (c) 1.2 Mrad, (d) 3.6 Mrad, and (e) 10 Mrad gamma irradiation doses.

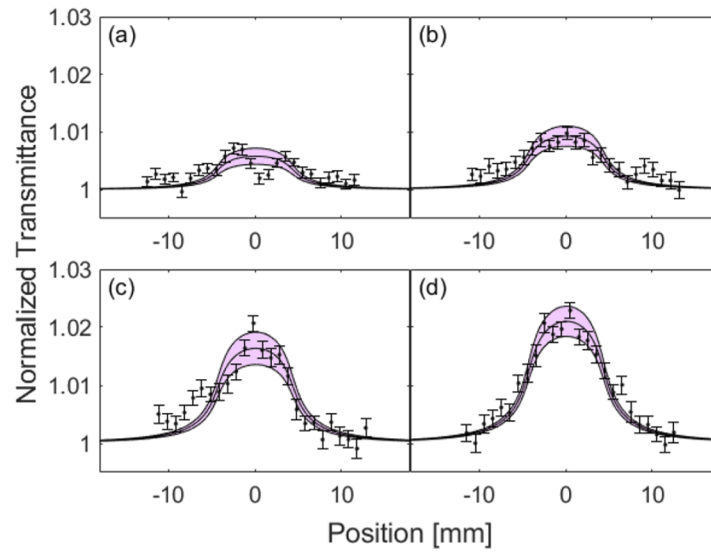


Fig. 5. Open-aperture Z-scan measurements of Infrasil302 thermally annealed to 200 °C after (a) 600 krad, (b) 1.2 Mrad, (c) 3.6 Mrad, and (d) 10 Mrad gamma irradiation doses.

Table 1. Nonlinear absorption coefficient β ($\times 10^{-13}$ m/W).

Gamma Dose	600 krad	1.2 Mrad	3.6 Mrad	10 Mrad
β : unannealed	-0.78 ± 0.06	-1.14 ± 0.12	-1.29 ± 0.11	-1.88 ± 0.06
β : annealed 200°C	-0.21 ± 0.05	-0.37 ± 0.07	-0.61 ± 0.10	-0.76 ± 0.09

Table 1 provides the measured β values for each gamma irradiation dose post-irradiation and after thermal annealing at 200 °C. The negative nonlinear absorption effect, which may be attributed to SA, increases in magnitude in Fig. 4 as the gamma dose increases. The increasing contribution of SA and resultant increased transmission through the sample with increasing gamma dose corresponds to an increasing absolute value of negative nonlinearity, as shown in

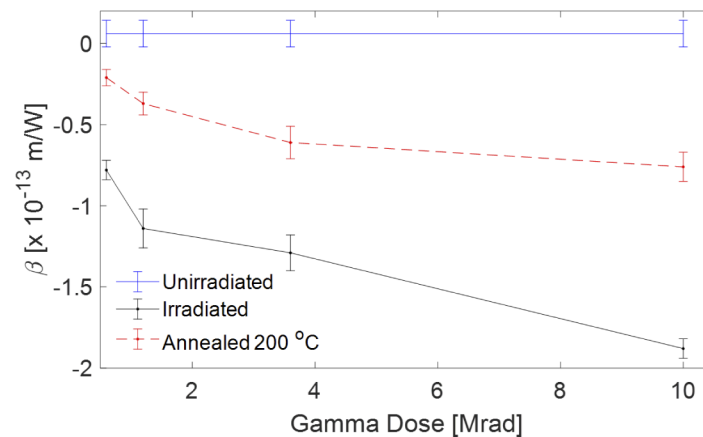


Fig. 6. Evolution of the Infrasil302 nonlinear absorption coefficient β with gamma dose and thermal annealing.

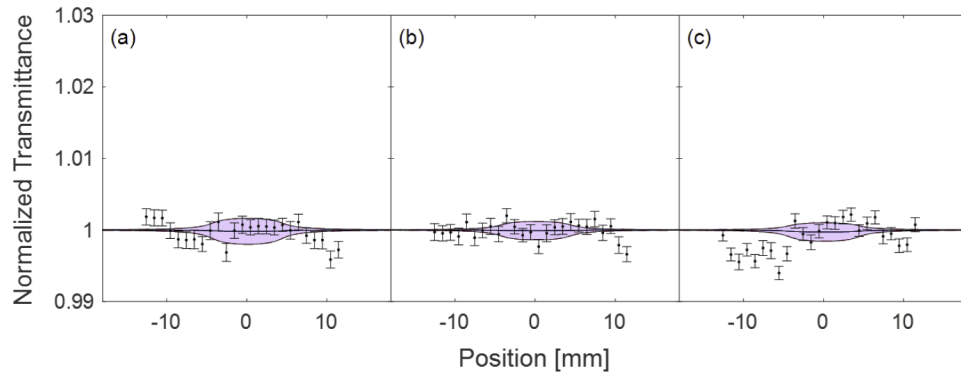


Fig. 7. Open-aperture Z-scan measurements of Infrasil302 concurrent-irradiation thermally annealed at 800 °C after (a) 600 krad, (b) 1.2 Mrad, and (c) 3.6 Mrad gamma irradiation doses.

Table 1. The change in the nonlinear absorption coefficient is nonlinear with increasing gamma dose and suggests the approach to a limit of the SA effect with increasing gamma dose.

Figure 5 shows the same irradiated Infrasil302 nonlinear absorption measurements as Fig. 4 after annealing to 200 °C for 30 minutes. The increased transmission attributed to the negative nonlinear absorption coefficient is shown to decrease with thermal annealing in all four cases. The nonlinear absorption is returned to the unirradiated state after annealing the samples to 400 °C for 30 minutes. The change of the nonlinear absorption coefficient with dose immediately after irradiation and after annealing to 200 °C for the four gamma doses is plotted in Fig. 6. In this plot the error bars represent the propagated error of the least squares fit used to calculate the nonlinear absorption coefficient. This plot further illustrates the nonlinear relationship between the increasing gamma dose and the nonlinear absorption.

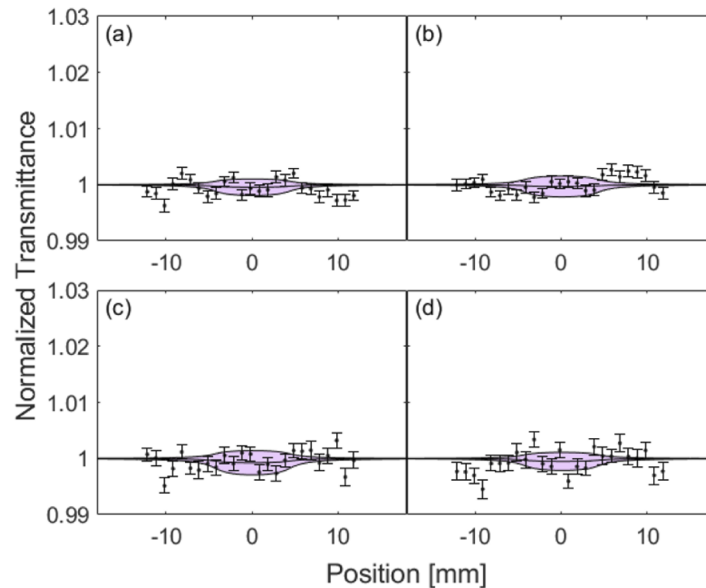


Fig. 8. Open-aperture Z-scan measurements of Spectrosil2000 (a) unirradiated, (b) 600 krad, (c) 1.2 Mrad, and (d) 3.6 Mrad gamma irradiation doses.

The 600 krad, 1.2 Mrad, and 3.6 Mrad gamma irradiations were repeated for Infrasil302 with concurrent-irradiation thermal annealing at 800 °C for the duration of the irradiation, and the z-scan measurements of nonlinear absorption for these irradiations are presented in Fig. 7. It can be seen that concurrent-irradiation thermal annealing maintained the Infrasil302 nonlinear absorption at its unirradiated state when compared to the plot in Fig. 4(a). Figure 8 shows the post-irradiation z-scan measurements of Spectrosil2000, equivalent to the measurements for Infrasil302 in Fig. 4, except for the 10 Mrad case. This figure shows that for the same irradiations, the nonlinear absorption coefficient of Spectrosil2000 remained unchanged and is discussed further in the conclusion section.

The linear absorption spectrum between 200 nm and 1100 nm for Infrasil302 quartz glass irradiated to 3.6 Mrad and annealed at temperatures of up to 800 °C is presented in Fig. 9 for

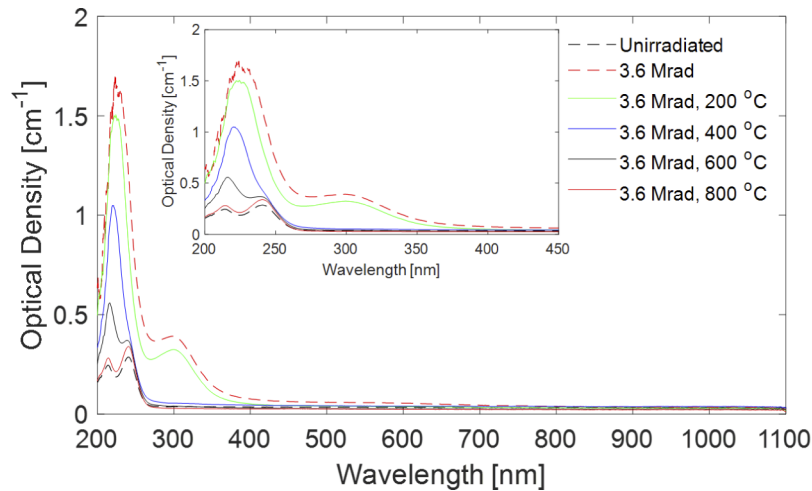


Fig. 9. Linear absorption of Infrasil302 when irradiated to 3.6 Mrad and annealed through 800 °C in 4 steps. Inset shows linear absorption from 200 nm to 450 nm.

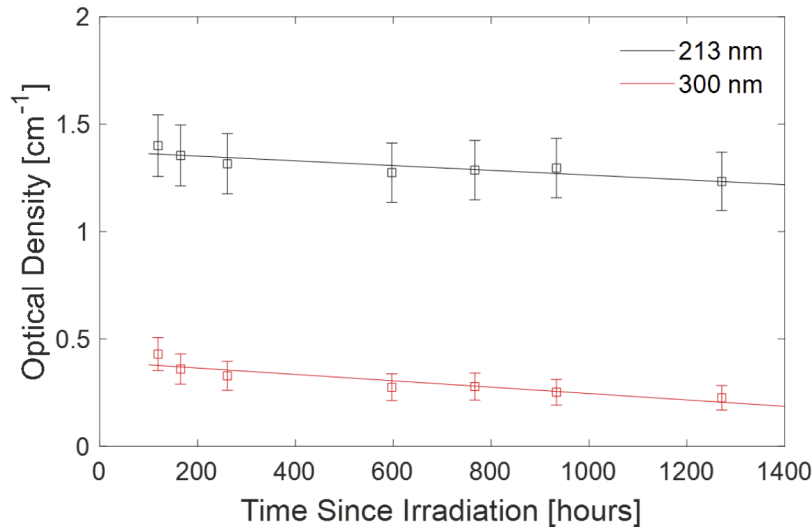


Fig. 10. Measured natural decay over time and fits for radiation-induced absorption peaks at 213 nm and 300 nm in an Infrasil302 sample irradiated to 500 krad gamma.

comparison with the measurements of nonlinear absorption. The expected absorption bands are observed at 213 nm and 300 nm, consistent with gamma irradiation electron defect generation and generation of Al impurity E' centers, respectively [17,18]. The radiation-induced linear absorption is shown to reduce to the unirradiated state after annealing to 800 °C. The spontaneous recovery of Infrasil302 was measured previously with a 500 krad gamma-irradiated sample evaluated five days after irradiation, and the results are presented in Fig. 10. The spontaneous recovery was evaluated for the radiation induced attenuation peaks at 213 nm and 300 nm and was found to decrease nonlinearly (exponentially). The linear absorption observed at 532 nm is consistent with the sample manufacturer's listed transmission within $\pm 1.5\%$ and decreases by 2% after irradiation to 3.6 Mrad. The unirradiated linear transmission of 91% and irradiated minimum linear transmission of 89% at 532 nm are sufficient to allow for the observed magnitude of SA-induced increase in transmission of up to 5% shown in Fig. 4.

4. Conclusion

A significant change of the nonlinear absorption coefficient of gamma-irradiated Infrasil302 has been measured by the open-aperture nanosecond Z-scan technique, which may be explained by the SA effect. Thermal annealing has also been shown to reduce the SA effect, ultimately restoring the quartz glass nonlinear optical properties to the unirradiated state at a temperature of 400 °C. The annealing has a similar effect on the linear absorption. SA is not typically observed in bulk optical materials, and understanding the relationship between SA and gamma dose in optical quartz glass is important for intense laser applications in radioactive environments.

Infrasil302 is a type I commercial silica glass manufactured by the electric melting of natural quartz crystal in vacuum or an inert gas at low pressure [19]. This process results in the presence of metallic impurities in the crystalline optical quartz glass. Heraeus Spectrosil2000, a type III synthetic fused silica manufactured by the hydrolyzation of SiCl_4 sprayed into an OH flame, is much purer than type I silica glass but has a higher water content [19]. We have subjected Spectrosil2000 to the same test as Infrasil302, as shown in Fig. 8, but did not witness the same negative radiation-induced nonlinearity. This suggests that the radiation-induced SA in Infrasil302 may be due to the metallic impurities, specifically aluminium ($\text{Al} \approx 20$ ppm), induced by the manufacturing process. Al-oxygen-hole-centers generated by gamma irradiation have been shown to cause an absorption band at 537 nm which may be responsible for the absorption and saturable absorption observed [18].

Funding. Department of Energy, Nuclear Science User Facilities (DE-NE0008906); U.S. Department of Defense (HDTRA1-20-2-0002); B. W. M (Army Advanced Civil Schooling Program).

Disclosures. The authors declare no conflicts of interest.

Data Availability. The data that support the findings of this study are available from the corresponding author upon reasonable request.

References

1. W. Primak and E. Edwards, "Radiation-induced dilatations in vitreous silica," *Phys. Rev.* **128**(6), 2580–2588 (1962).
2. W. Primak and J. Luthra, "Radiation induced expansion and increase in refractive index of magnesium oxide; evidence for the F center," *Phys. Rev.* **150**(2), 551–561 (1966).
3. W. Primak and R. Kampwirth, "The radiation compaction of vitreous silica," *J. Appl. Phys.* **39**(12), 5651–5658 (1968).
4. E. V. Stryland and M. Shiek-Bahae, *Z-Scan Measurements of Optical Nonlinearities* (Marcel Dekker, Inc., 1998).
5. T. Olivier, F. Billard, and H. Akhouayri, "Z-scan theoretical and experimental studies for accurate measurements of the nonlinear refractive index and absorption of optical glasses near damage threshold," *Proc. SPIE* **5273**, 341–349 (2004).
6. J. Wang, B. Gu, H.-T. Wang, and X.-W. Ni, "Z-scan analytical theory for material with saturable absorption and two-photon absorption," *Opt. Commun.* **283**(18), 3525–3528 (2010).
7. T. Olivier, F. Billard, and H. Akhouayri, "Z-scan studies of the nonlinear refractive index of fused silica in the nanosecond regime," *Proc. SPIE* **5252**, 391–401 (2004).

8. M. Sheik-bahae, A. A. Said, and E. V. Stryland, "High-sensitivity, single-beam n_2 measurements," *Opt. Lett.* **14**(17), 955–957 (1989).
9. L. L. Chase and E. W. V. Stryland, *Handbook of Laser Science and Technology Supplement 2: Optical Materials* (CRC Press, New York, 1995), vol. 2, pp. 269–366, 5th ed.
10. A. Dragomir, J. G. McInerney, and D. N. Nikogosyan, "Two-photon absorption properties of commercial fused silica and germanosilicate glass at 264 nm," *Appl. Phys. Lett.* **80**(7), 1114–1116 (2002).
11. A. Scalisi, G. Compagnini, L. D'Urso, and O. Puglisi, "Nonlinear optical activity in Ag–SiO₂ nanocomposite thin films with different silver concentration," *Appl. Surf. Sci.* **226**(1-3), 237–241 (2004).
12. Y.-L. Huang, C.-K. Sun, J.-C. Liang, S. Keller, M. P. Mack, U. K. Mishra, and S. P. DenBaars, "Femtosecond z-scan measurement of GaN," *Appl. Phys. Lett.* **75**(22), 3524–3526 (1999).
13. J. Olesiak-Banska, M. Waszkielewicz, K. Matczyszyn, and M. Samoc, "A closer look at two-photon absorption, absorption saturation and nonlinear refraction in gold nanoclusters," *RSC Adv.* **6**(101), 98748–98752 (2016).
14. V. Sreeja, A. Cheruvalathu, R. Reshmi, E. Anila, S. Thomas, and M. Jayaraj, "Effect of thickness on nonlinear absorption properties of graphite oxide thin films," *Opt. Mater.* **60**, 450–455 (2016).
15. T. Miyoshi, N. Matsuo, P. Maly, F. Trojanek, P. Nemec, and J. Kudrna, "Negative and positive nonlinear absorption in CdS-doped glasses," *J. Mater. Sci. Lett.* **20**(4), 343–345 (2001).
16. B. W. Morgan, M. V. Zile, P. Sabharwall, M. Burger, and I. Jovanovic, "Post-irradiation examination of optical components for advanced fission reactor instrumentation," *Rev. Sci. Instrum.* **92**(10), 105107 (2021).
17. C. D. Marshall, J. A. Speth, and S. A. Payne, "Induced optical absorption in gamma, neutron and ultraviolet irradiated fused quartz and silica," *J. Non-Cryst. Solids* **212**(1), 59–73 (1997).
18. H. Hosono and K. Hiroshi, "Radiation-induced coloring and paramagnetic centers in synthetic SiO₂:Al glasses," *Nucl. Instrum. Methods Phys. Res., Sect. B* **91**(1-4), 395–399 (1994).
19. R. Kitamura, L. Pilon, and M. Jonasz, "Optical constants of silica glass from extreme ultraviolet to far infrared at near room temperature," *Appl. Opt.* **46**(33), 8118–8133 (2007).